

# INTERNATIONAL SOCIETY FOR SOIL MECHANICS AND GEOTECHNICAL ENGINEERING



*This paper was downloaded from the Online Library of the International Society for Soil Mechanics and Geotechnical Engineering (ISSMGE). The library is available here:*

<https://www.issmge.org/publications/online-library>

*This is an open-access database that archives thousands of papers published under the Auspices of the ISSMGE and maintained by the Innovation and Development Committee of ISSMGE.*

*The paper was published in the proceedings of the 7<sup>th</sup> International Conference on Earthquake Geotechnical Engineering and was edited by Francesco Silvestri, Nicola Moraci and Susanna Antonielli. The conference was held in Rome, Italy, 17 - 20 June 2019.*

# Cyclic simple shear testing for assessing liquefaction mitigation by fibre reinforcement

S. Robinson, A.J. Brennan, J.A. Knappett & K. Wang  
*School of Science and Engineering, University of Dundee, Dundee, UK*

A.G. Bengough  
*The James Hutton Institute, Invergowrie, UK*  
*School of Science and Engineering, University of Dundee, Dundee, UK*

**ABSTRACT:** Earthquake induced soil liquefaction represents a significant hazard. Fibre reinforcement, whether by artificial fibres or plant roots, has been suggested as a potential method for mitigating soil liquefaction and has shown promise in a number of physical modelling studies. However, the mechanism by which the fibres work to counteract liquefaction is not yet well understood. This work describes a programme of Cyclic Simple Shear (CSS) testing on HST 95 sand with Loksand synthetic fibres undertaken to investigate this mechanism and improve understanding. The results suggest that the addition of fibres does not prevent or delay the occurrence of liquefaction, but most likely restrains the large deformations which would occur after the soil has liquefied.

## 1 INTRODUCTION

### 1.1 *Background and current understanding*

The use of fibre reinforcement in soil, whether artificially added or by the use of fibrous roots, is the subject of much current research in Geotechnical Engineering (Meijer et al., 2018a; Liang and Knappett, 2017a; Wang and Brennan, 2015; Ibraim et al., 2010). Its benefits in large displacement problems such as slope stability are now well proven (Liang and Knappett, 2017b), however, the behaviour of fibre reinforcement in the case of earthquake induced liquefaction is more poorly understood. Research to date has focussed on centrifuge modelling, shaking table tests and triaxial testing. The benefits of fibre reinforcement during liquefaction have been shown by a number of studies where it has been found that the use of fibres can minimise quay wall movement (Wang and Brennan, 2015) and also pipeline uplift (Wang et al., 2018) for example.

Whilst physical modelling research is key to highlighting these benefits, element testing plays an important role in identifying the fundamental mechanism by which fibre reinforcement works during liquefaction. The element testing of fibre reinforced specimens conducted to investigate liquefaction to date has been based entirely on triaxial testing (Ibraim et al., 2010; Noorzad and Fardad Amini, 2014; Fardad Amini and Noorzad, 2018). Whilst this is undoubtedly useful, the question should be asked whether the mode of shearing which occurs in triaxial testing (deviatoric shear) causes differences in results compared to the shearing mechanism which occurs in the field. Whilst Cyclic Simple Shear (CSS) testing is commonly used to assess the liquefaction potential of sands (eg Porcino and Diano, 2016; Monkul et al., 2015), CSS testing which arguably represents a shearing mechanism far closer to field conditions has never before been conducted to assess liquefaction of fibre reinforced specimens. This paper sets out a programme of CSS testing to assess the performance of fibre reinforcement as a method to mitigate liquefaction in sand and the subsequent consequences.

## 2 METHODOLOGY

### 2.1 *Experimental setup*

The cyclic simple shear tests were conducted using an electro-mechanical GDS Instruments Variable Direction Dynamic Simple Shear Device (VDDCSS) as shown in Figure 1a. The system is capable of applying combinations of shear (horizontal) forces in two directions whilst also controlling the axial (vertical) force on the soil specimen, although for this testing programme only one horizontal axis was used. The specimen itself (70 mm diameter and 24 mm in height) is housed in a series of 1 mm high Teflon coated steel rings surrounding a latex membrane, with two porous stainless-steel interface discs at the top and bottom of the specimen which transmit the shear forces (Fig. 1b). The base pedestal is mounted on two sets of linear bearings and is connected to two 2 kN load cells (one for each horizontal axis) allowing independent  $\pm 10$  mm travel in each direction. The top interface is attached to a two-axis shear force cell, which directly measures the shear force applied to the specimens such that additional resistance from the linear bearings does not require to be accounted for. Axial force on the specimen is applied by a further electro-mechanical actuator via a 5 kN load cell directly above the shear force cell and loading frequencies of up 1 Hz are possible on all axes.

A key requirement in the study of liquefaction is the ability to maintain constant specimen volume during shearing to represent undrained conditions. Whilst in conventional CSS apparatus this is done by mechanically locking the height of the top interface, the system used here maintains constant height by means of a high speed (10,000 Hz) feedback loop between a local axial LVDT (Linear Variable Differential Transformer) measuring the specimen height and the axial actuator. This approach minimises the effect of compliance from the axial actuator. A further two local LVDTs measure the shear displacements in each horizontal axis. The LVDTs have a measurement range of  $\pm 1.5$  mm and a resolution of  $0.1 \mu\text{m}$ . The VDDCSS has an internal data acquisition system which measures each transducer and connects by USB to a PC running GDSLAB software used to control the system.

### 2.2 *Specimen preparation*

A number of methods for preparing the fibre reinforced sand specimens were considered including air pluviation (Wang et al., 2018) and sample vibration (Ibraim et al., 2012), however, the only approach which created repeatable specimens for these samples was moist compaction. This is the most commonly used method for preparing specimens of this nature (Ibraim et al., 2010). To ensure a uniform specimen, compaction was carried out in two 12

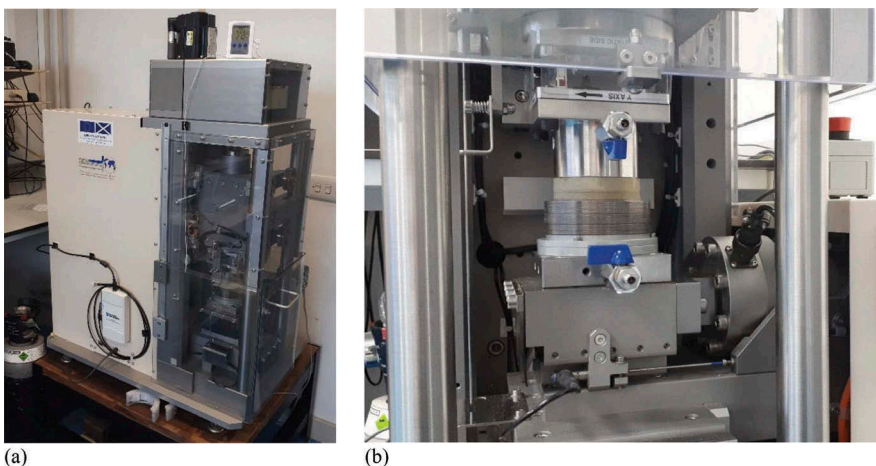


Figure 1. (a) VDDCSS system and (b) the specimen housed within Teflon coated rings.

Table 1. Properties of HST 95 sand.

Property	Value
$D_{10}$ (mm)	0.10
$D_{50}$ (mm)	0.14
Coefficient of uniformity, $C_u$	2.25
Coefficient of curvature, $C_c$	1.36
Critical state friction angle (degrees)	32
Maximum dry density ( $\text{kg/m}^3$ )	1792
Minimum dry density ( $\text{kg/m}^3$ )	1487

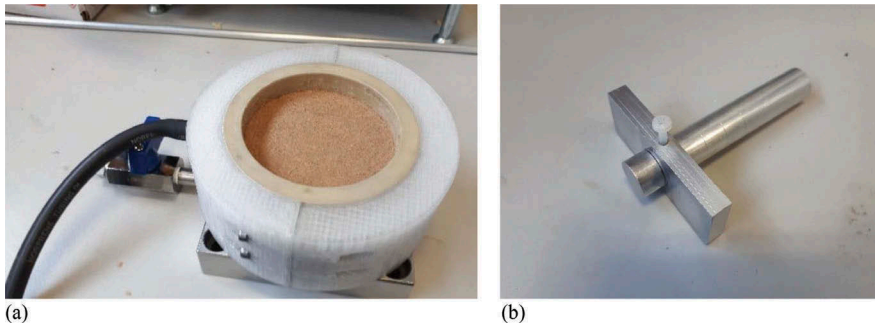


Figure 2. (a) 3D printed vacuum mould and (b) compaction tool for specimen preparation.

mm thick layers. Following the method described by Ibraim et al. (2010), HST 95 sand (Table 1) was prepared at its optimal moisture content for compaction ( $w = 9\%$ ) and mixed with crimped LokSand™ polypropylene fibres (35 mm in length and 0.1 mm in diameter, with a Young's modulus of 900 MPa) at a ratio of 0.6 % by weight. The fibres were added to the moist sand in small amounts whilst stirring the sand to distribute them evenly.

A custom designed 3D printed vacuum mould (Fig. 2a) was used to hold the latex membrane securely against the inside of the Teflon coated rings during specimen preparation. The latex membranes themselves were custom made in-house to exactly match the inner diameter of the rings, as the 70 mm diameter triaxial membranes commonly used are designed to be significantly smaller than 70 mm in diameter such that they fit tightly to a triaxial specimen. In the case of the thin (24 mm high) sand specimens used here this was observed to noticeably affect the specimens, causing a reduction in diameter and increase in height when the vacuum was removed during installation. Next the sand-fibre mixture was placed into the mould and compacted using a cylindrical compaction tool 20 mm in diameter, with a stop such that over-compaction beyond a set height was not possible (Fig. 2b). This was repeated for the second layer before the vacuum was removed and the specimen was secured to the base pedestal.

It is important to note that as the specimens are moist compacted, they are partially saturated. To remove this effect, the specimens were saturated using de-aired water from a GDS Standard Digital Pressure Controller (STDDPCv2). To achieve this, the pressure controller was connected to the porous stainless-steel platen at the base of the specimen whilst the valve from the top porous platen was open such that it vented to atmospheric pressure. A pressure differential of 1 kPa was applied such that saturation occurred over 1 hour, whilst a vertical stress of 5 kPa was maintained using the vertical actuator. After this point, the base valve was closed and the pressure controller was disconnected. The top drainage valve was kept open throughout testing such that no pore pressure was allowed to develop in the specimen. The specimen was then consolidated to a vertical effective stress of 25 kPa which was maintained for a period of 2 hours before shearing. The tests were conducted using the equivalent undrained method described by Montoya et al. (2013) where the CSS tests are conducted

Table 2. Programme of Cyclic Simple Shear (CSS) testing.

Test No.	$D_r$ (%)	$\sigma'_{v0}$ (kPa)	CSR	Interface	$w_f$ (%)
1	40	25	0.04	Pins	0
2	40	25	0.04	Pins	0.6
3*	40	25	0.04	Pins	0.6
4	40	25	0.08	Pins	0
5	40	25	0.08	Pins	0.6
6	40	25	0.19	Pins	0
7	40	25	0.19	Pins	0.6
8	40	25	0.08	Flat	0

\* Test 3 is a repeat of Test 2.

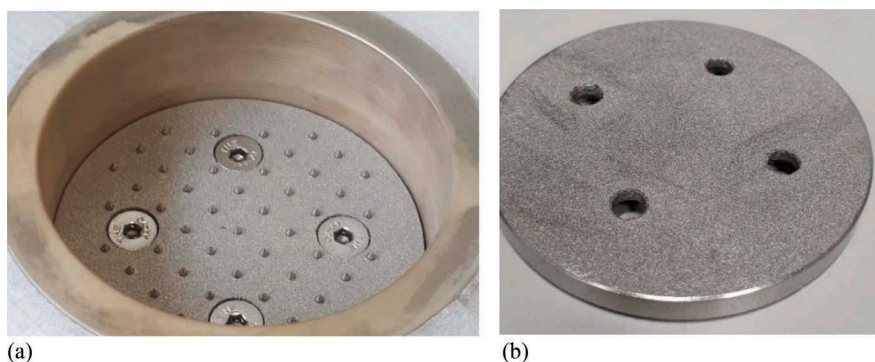


Figure 3. Porous stainless-steel interface discs used (a) with pins and (b) with a flat surface.

under drained constant volume conditions and the corresponding undrained pore pressure is calculated from the loss of the measured axial stress. This approach has been used by several studies including Monkul et al. (2015) and Porcino and Diano (2016).

### 2.3 Test programme

The testing programme (Table 2) was designed to match as closely as possible the conditions from Wang et al. (2018) in which the impact of fibre reinforcement on liquefaction induced pipeline uplift was investigated. The tests were all conducted at a relative density ( $D_r$ ) of 40 %, whilst the 25 kPa initial vertical effective stress used was selected to represent the mid-height point of the centrifuge models. Similarly, the cyclic stress ratios (CSR) were selected to match the measured accelerations at the same point in the centrifuge models. Two types of interface were used; flat porous discs and a new porous disc with pin interfaces with the specimen (Fig. 3). The comparison between the fibre reinforced ( $w_f = 0.6$  %) and unreinforced ( $w_f = 0$  %) specimens was conducted using the pin interface type, as this was designed to allow positive engagement with the fibre reinforcement without disturbing the top surface of the specimen.

## 3 RESULTS

### 3.1 Comparison of interface types

Before considering the effect of fibre reinforcement on the liquefaction response of the specimens, a validation of the pinned interface is first presented to demonstrate its equivalence to

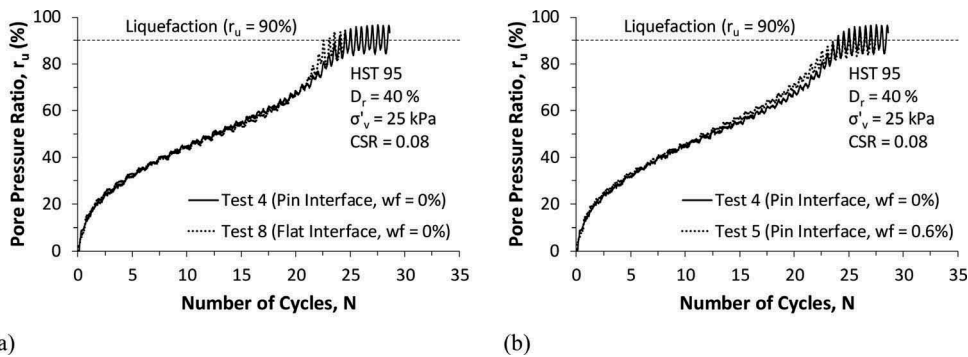


Figure 4. (a) Comparison between the two interface types used and (b) comparison between fibre reinforced and unreinforced specimens at 40% relative density and  $CSR = 0.08$ .

the flat interface commonly used. Test 8 was conducted under the same conditions as Test 4 (with the exception of the interface) allowing comparison to be made. Figure 4a shows the result of these two tests in terms of the evolution of the pore pressure ratio,  $r_u$ , with the number of cycles of loading. The response is similar throughout, with both specimens reaching liquefaction ( $r_u = 90\%$ ) between 23 and 24 cycles. This suggests that the new pinned interface provides comparable results to the conventional flat interface.

### 3.2 Effect of fibre reinforcement

Figure 4b shows a comparison of the tests conducted at  $CSR = 0.08$  with and without fibre reinforcement as an example. No significant differences between the specimens were observed, with both specimens evolving pore pressure in a similar manner and 90 % liquefaction occurring at 25 and 24 cycles respectively. This suggests that the addition of the fibre reinforcement does not prevent the occurrence of liquefaction. Similar findings can be seen across the values of  $CSR$  tested (Fig. 5a and Table 3). Slightly more variability was observed in the fibre reinforced specimens at  $CSR = 0.04$ , hence this test was repeated. Figure 5b shows the variation of the number of cycles required to induce liquefaction,  $N_{liq}$ , with  $CSR$  which clearly show  $N_{liq}$  reducing with increasing  $CSR$ . Tests conducted at  $CSR = 0.04$  reached full liquefaction at 1500 cycles on average, whilst the tests at  $CSR = 0.19$  liquefied within the first loading cycle. A small improvement is observable at  $CSR = 0.19$ , where the fibre reinforced specimen liquefied at 1.0 cycles compared to 0.5 cycles for the unreinforced specimen.

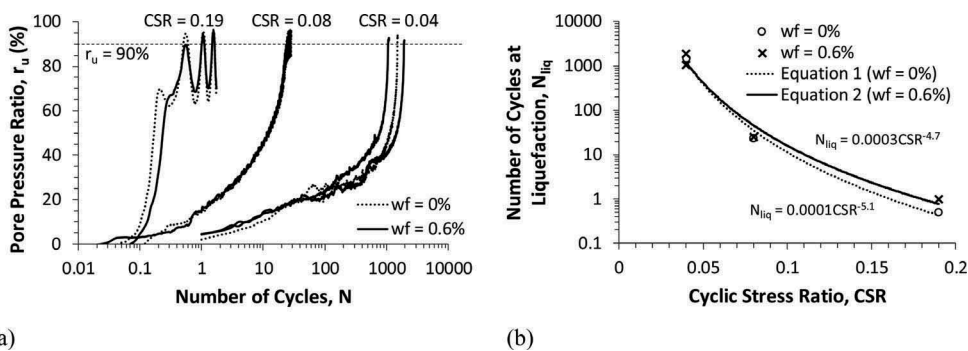


Figure 5. (a) Comparison of the evolution of pore pressure ratio between fibre reinforced and unreinforced specimens at each  $CSR$  and (b) the influence of  $CSR$  on the number of cycles at liquefaction ( $r_u = 90\%$ ).

Table 3. Summary of results of Cyclic Simple Shear testing.

Test No.	CSR	$w_f$ (%)	$N_{liq}$	$\gamma_{cyc,liq}$
1	0.04	0	1506	0.0014
2	0.04	0.6	1066	0.0014
3*	0.04	0.6	1924	0.0013
4	0.08	0	24	0.0023
5	0.08	0.6	25	0.0029
6	0.19	0	0.5	0.0090
7	0.19	0.6	1.0	0.0085

\* Test 3 is a repeat of Test 2.

#### 4 DISCUSSION

At first inspection, the results suggest fibre reinforcement is not useful in preventing the occurrence of liquefaction, however, this is in contrast to a number of studies. Wang et al. (2018) demonstrated using a geotechnical centrifuge that the inclusion of fibres can reduce liquefaction induced pipeline uplift, while cyclic triaxial testing studies such as Fardad Amini and Noorzad (2018) showed that the addition of fibres increased the number of cycles required to cause liquefaction of sand specimens. A possible explanation for this discrepancy can be found in Fardad Amini and Noorzad (2018) which showed that differences in pore pressure ratio evolution can be seen only after 60 to 80 % liquefaction ( $r_u = 0.6$  to 0.8) has already occurred. As the cyclic strain amplitude increases significantly beyond this point (Fig. 6), this could be expected to be the point at which additional resistance from the fibres begins to mobilise. This would suggest that the fibre reinforcement primarily acts by restraining large deformations which occur after most of the liquefaction has already occurred. Further evidence of this can be seen in Noorzad and Fardad Amini (2014) and Ibraim et al. (2010) which demonstrated that unreinforced triaxial specimens collapse after liquefaction, whilst fibre reinforced specimens do not and instead retain their shape.

If fibre reinforcement primarily works to restrain deformation after liquefaction rather than preventing liquefaction itself, then a key consideration should be the strain level required to mobilise additional resistance from the fibre reinforcement. The need for a certain strain to occur before root or fibre reinforcement begins to mobilise is discussed in Meijer et al. (2018a). Examination of the monotonic triaxial testing of fibre reinforced sand specimens by Ibraim et al. (2010) suggests that a shear strain of 1 to 2 % is required before any noticeable reinforcing effect is observed. This would explain why no beneficial effect of the fibres was observed in this study, as the strain levels at which liquefaction was found to occur ranged

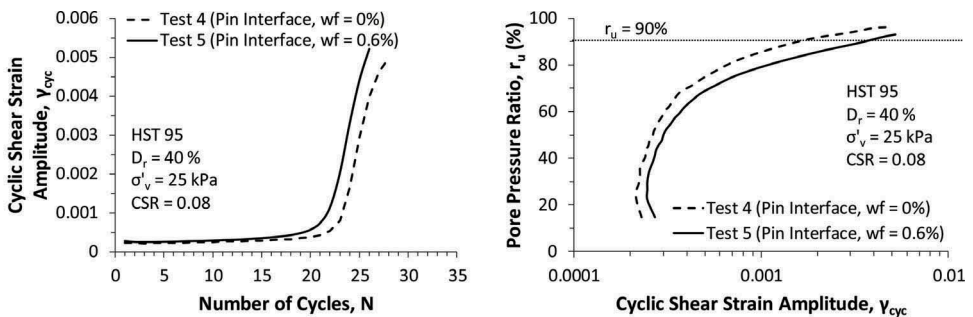


Figure 6. (a) Change in the cyclic shear strain amplitude with number of cycles and (b) variation of the pore pressure ratio with cyclic shear strain amplitude, both for CSR = 0.08.

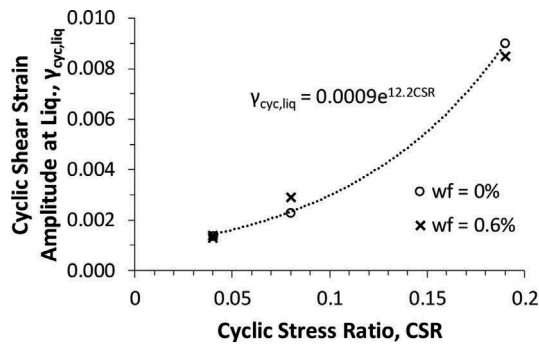


Figure 7. Variation of the cyclic shear strain amplitude at liquefaction with CSR.

from 0.1 to 0.9 % shear strain for the CSS tests conducted (Fig. 7). This is significantly below the 1 to 2 % strain expected to be required to mobilise the fibre reinforcement, meaning that liquefaction has already occurred before the fibres can provide any benefit. It is also important to note that Ibraim et al. (2010) used LokSand™ fibres similar to those used in this study.

The next question that arises is why reinforcing effects are observed in triaxial testing of fibre reinforced specimens, but not in the CSS testing conducted here. A reason for this can be found in Dobry and Abdoun (2015) which considered differences in the strain required for liquefaction between triaxial studies and field data. It was shown that value of  $\gamma_{cyc,liq}$  from these element tests ranged from 0.3 to 4 % shear strain for strain controlled triaxial tests and 3 to 50 % shear strain for stress controlled triaxial tests. Both of these ranges exceed the 1 to 2 % shear strain suggested by data from Ibraim et al. (2010) required to mobilise fibre reinforcement. This would mean that the fibre reinforcement would mobilise before full liquefaction occurs in the triaxial specimens. For the field data, large scale tests and centrifuge testing, liquefaction was suggested to occur at 0.06 to 0.12 % shear strain, which is significantly lower than the range found in triaxial testing, raising the question of whether the effect of fibre reinforcement increasing the liquefaction resistance of the triaxial specimens would actually be observed in the field. The strain at liquefaction from the CSS tests conducted here (0.1 to 0.9 % shear strain) is closer to the range suggested from field data, suggesting that CSS testing may be a more appropriate method for assessing liquefaction behaviour than triaxial testing, potentially due to the similarities in the shearing mechanism compared to the field behaviour.

Finally, it is important to consider the findings of this testing programme on synthetic fibres in terms of the response of real fibrous roots. Whilst the synthetic fibres used are similar to fine fibrous roots in terms of their physical dimensions, they differ in terms of the Young's modulus. The Loksand™ fibres are made of polypropylene and have a Young's modulus of 900 MPa, compared to a typical Young's modulus of approximately 50 to 200 MPa for fibrous roots of a similar diameter (Loades et al., 2012; Meijer et al., 2018b). The lower modulus of real fibrous roots would suggest that greater shear strains would be required to mobilise the real roots, and that for a given shear strain, the additional root reinforcement would be lower. Hence, shear strains greater than the value of 1 to 2 % suggested by Ibraim et al. (2010) (where Loksand™ fibres were also used) could be required to begin to mobilise the resistance of fibrous roots. The consequence of this is that the use of synthetic fibres (which have a greater modulus) in element testing could lead to an overestimation of reinforcing effects in real fibrous roots.

## 5 CONCLUSIONS

This paper has investigated the use of fibre reinforcement as a liquefaction countermeasure using Cyclic Simple Shear (CSS) testing, which has not been previously attempted. A number of key findings have arisen from the research.

- Comparison between the fibre reinforced and unreinforced specimens suggests that fibre reinforcement does not have an impact on the occurrence of liquefaction itself. This is due to the fact that 1 to 2 % shear strain is needed to mobilise the fibres, by which point liquefaction has already occurred.
- The benefits of fibre reinforcement for liquefaction mitigation reported by physical modelling studies most likely come from the fibres restraining and minimising the large deformations which occur after liquefaction.
- CSS testing may be a more appropriate method to assess the usefulness of fibres during liquefaction than triaxial testing due to the similarity in shearing mechanism compared to the field conditions.

## ACKNOWLEDGEMENTS

This work has been supported by funding from the Leverhulme Trust (Grant No. RPG-2015-091) which is gratefully acknowledged.

## REFERENCES

- Dobry, R. & Abdoun, T.2015. Cyclic shear strain needed for liquefaction triggering and assessment of overburden pressure factor  $K_\sigma$ . *Journal of Geotechnical and Geoenvironmental Engineering*141(11): 1–18.
- Fardad Amini, P. & Noorzad, R.2018Energy-based evaluation of liquefaction of fiber-reinforced sand using cyclic triaxial testing. *Soil Dynamics and Earthquake Engineering*104: 45–53.
- Ibraim, E., Diambra, A., Muir Wood, D & Russell, A.R.2010. Static liquefaction of fibre reinforced sand under monotonic loading. *Geotextiles and Geomembranes*28:374–385.
- Ibraim, E., Diambra, A., Russell, A.R. & Muir Wood, D.2012. Assessment of laboratory sample preparation for fibre reinforced sands. *Geotextiles and Geomembranes*34: 69–79.
- Liang, T. & Knappett, J.A.2017a. Newmark sliding block model for predicting the seismic performance of vegetated slopes. *Soil Dynamics and Earthquake Engineering*101: 27–40.
- Liang, T. & Knappett, J.A.2017b. Centrifuge modelling of the influence of slope height on the seismic performance of rooted slopes. *Geotechnique*67(10): 855–869.
- Loades, K.W., Bengough, A.G., Bransby, M.F. and Hallett, P.D.2012. Biomechanics of nodal, seminal and lateral roots of barley: effects of diameter, waterlogging and mechanical impedance. *Plant and Soil*370 (1-2): 407–418.
- Meijer, G.J., Bengough, A.G., Knappett, J.A., Loades, K.W. and Nicoll, B.C.2018a. In situ measurement of root reinforcement using corkscrew extraction method. *Canadian Geotechnical Journal*55: 1372–1390.
- Meijer, G.J., Bengough, G., Knappett, J., Loades, K. and Nicoll, B.2018b. In situ root identification through blade penetrometer testing – part 2: field testing. *Geotechnique*68(4): 320–331.
- Monkul, M.M., Gültekin, C., Güllver, M., Akin, Ö. & Eseller-Bayat, E.2015. Estimation of liquefaction potential from dry and saturated sandy soils under drained constant volume cyclic simple shear loading. *Soil Dynamics and Earthquake Engineering*75: 27–36.
- Montoya, B.M., DeJong, J.T. & Boulanger, R.W.2013. Dynamic response of liquefiable sand improved by microbial-induced calcite precipitation. *Geotechnique*63(4): 302–312.
- Noorzad, R. & Fardad Amini, P.2014. Liquefaction resistance of Babolsar sand reinforced with randomly distributed fibers under cyclic loading. *Soil Dynamics and Earthquake Engineering*66: 281–292.
- Porcino, D. & Diano, V.2016. Laboratory study on pore pressure generation and liquefaction of low-plasticity silty sandy soils during the 2012 earthquake in Italy. *Journal of Geotechnical and Geoenvironmental Engineering*142(10): 1–10.
- Wang, K. & Brennan, A.J.2015. Centrifuge modelling of fibre-reinforcement using as a liquefaction countermeasure of quay wall backfill. In *Proceedings of the 6<sup>th</sup> International Conference on Earthquake Geotechnical Engineering*, Christchurch, NZ, 1–4 November 2015.
- Wang, K., Brennan, A.J., Knappett, J.A., Robinson, S. & Bengough, A.G.2018. Centrifuge modelling of remediation of liquefaction-induced pipeline uplift using model root systems. In McNamara et al. (eds), *Physical Modelling in Geotechnics*: 1265–1270. London: Taylor & Francis Group.